

Probing Defects in MoS₂ Van der Waals Crystal through Deep-Level Transient Spectroscopy

Łukasz Gelczuk,* Jan Kopaczek, Paweł Scharoch, Katarzyna Komorowska, Mark Blei, Sefaattin Tongay,* and Robert Kudrawiec*

The electrical performance of transition metal dichalcogenides (TMDCs) is strongly affected by the quality of electrical metal contacts and the formation of electrically active defects. Herein, deep-level transient spectroscopy (DLTS) is used for direct probing of deep-level defects in the bandgap of single MoS₂ van der Waals crystal. Standard DLTS temperature spectra reveal a deep-level trap located at about 0.36 eV below the conduction band edge. This trap is tentatively attributed to sulfur vacancies and localized on the electronic band structure of MoS₂, obtained within the density functional theory (DFT), and matched with experimentally studied electronic band structure, by absorption and contactless electroreflectance (CER) spectroscopy.

The transition metal dichalcogenides (TMDCs) such as MoS_2 , $MoSe_2$, WSe_2 , and so on are emerging family of 2D layered materials similar to graphene, which are considered as promising candidates for various modern nanoelectronic and optoelectronic ultrathin device applications.^[1-3] In TMDCs, one unit layer has a common form of MX_2 (M = Mo or W and X = S or Se). The intralayer bonds are strong covalent bonds, whereas the interlayer bonds between two MX_2 slabs are typically weak van der Waals (VdW) bonds, which allow micromechanical exfoliation of TMDCs down to single or few layers.^[4] Single or multilayer TMDCs exhibit numerous fascinating properties

Dr. Ł. Gelczuk
Faculty of Microsystem Electronics and Photonics
Wroclaw University of Science and Technology
Janiszewskiego 11/17, Wroclaw 50-372, Poland
E-mail: lukasz.gelczuk@pwr.edu.pl

Dr. J. Kopaczek, Dr. P. Scharoch, Prof. R. Kudrawiec Faculty of Fundamental Problems of Technology Wrocław University of Science and Technology Wybrzeże Wyspiańskiego 27, Wrocław 50-370, Poland E-mail: robert.kudrawiec@pwr.edu.pl

Dr. K. Komorowska, Prof. R. Kudrawiec Łukasiewicz Research Network PORT Polish Center for Technology Development Stabłowicka 147, Wrocław 54-066, Poland

M. Blei, Prof. S. Tongay School for Engineering of Matter, Transport and Energy Arizona State University Tempe, AZ 85287, USA E-mail: Sefaattin.Tongay@asu.edu

The ORCID identification number(s) for the author(s) of this article can be found under https://doi.org/10.1002/pssr.202000381.

DOI: 10.1002/pssr.202000381

associated with their reduced thickness. Unlike graphene, which does not have a bandgap in its pristine form, the TMDCs can exhibit both metallic and semiconducting properties through the proper selection of metal or chalcogen in the crystal, and their bandgaps are tunable with thickness. Namely, bulk MoS₂ is a semiconductor with an indirect bandgap of about 1.2 eV. When its thickness is reduced to a few layers, the indirect bandgap is tuned by quantum confinement and increases substantially to about 1.3 eV and more, until it eventually exceeds the energy spacing of the direct gap for monolayer (ML) thickness. Finally, ML

MoS₂ shows a direct bandgap of about 1.8 eV. [5]

It is generally known that in semiconductors intrinsic structural defects (e.g., vacancies, interstitials, antisites, and so on) can act as very efficient traps for electrons or holes and they can strongly influence transport and electrooptical properties of the host material. Although the understanding of defects in conventional 3D semiconductors is well established and the defects database is relatively complete, physics and activity of defects in 2D semiconductors, such as the family of layered semiconducting TMDCs, are still a field under investigation.^[6] Because of their physical dimensions, 2D materials are very sensitive to the presence of defects in their crystalline structure. Beyond 2D defects (i.e., vdW solids, layer stacking of different layers, folding and wrinkling of layers, and so on), as well as 1D defects (i.e., grain boundaries, edges, in-plane heterolayers, and so on), also many types of 0D defects (vacancies, adatoms, substitutional impurities, etc.) can be observed in TMDC crystals. [6] In contrast to graphene, which is made of only one layer of carbon, the alternating X-M-X increases the variety of point defects in TMDCs. The influence of defects on the properties of TMDCs has been extensively studied in recent years both theoretically and experimentally. [6-17] Atomic (chalcogen or metal) vacancies are regarded as the most common point defects in TMDCs and are known to induce profound modification of their electronic structure. In case of MoS₂, first-principles calculations based on density functional theory (DFT) predict the prevalence of sulfur vacancies (V_S) against all the other types of point defects (e.g., antisites, interstitials, or Mo-vacancies), both in the ML and in the bulk crystal. [7–10] Direct experimental evidence that sulfur vacancies exist in MoS2 has been obtained from high-resolution transmission electron microscopy (TEM).[7,11] Preliminary DFT calculations have indicated that V_S introduce localized donor



states in the bandgap, causing unpaired electrons into the lattice and n-type doping the material.[11] This was consistent with experimentally observed n-type conductivity in MoS2-based field-effect transistors (FET). [1–3] Localized electronic states created around V_S have also been indicated to be responsible for charge transport mechanism at low carrier density regime by hopping between these localized defect states.^[11] Similar to sulfur-deficient MoS₂ also sulfur-rich (or molybdenum-deficient) MoS₂ would be expected to result in p-type doping. Indeed, local n-type and p-type charge transports have been identified even in different regions of the same MoS2 sample, suggesting that the local stoichiometry might vary significantly from the average macroscopic stoichiometry. [12] However, extensive DFT calculations showed that the most abundant native defect V_S in bulk or ML MoS₂ is either in neutral or negative charge state.^[8,9] Thus, being deep acceptor it cannot be the cause of the observed n-type doping. In fact, the n-type doping of MoS₂ is usually assigned to Re impurities, which are often present in natural samples but not in the synthetic ones. Nb atoms, in turn, are considered as p-type dopants. [6] The native defect, such as V_s, cannot be efficient n-type dopant in MoS2, but it can still act as a deep electron trap center, by which the electrical conductivity in MoS2-based electronic devices can be partly suppressed in the presence of native compensation defects.[8]

Deep-level transient spectroscopy (DLTS) is normally used to measure the electrical properties of deep-level defects in bulk semiconductor crystals or epitaxial layers. However, this technique has some crucial limitations and special requirements for ML samples. Its application is difficult for defect characterization in 2D materials and thus other optical spectroscopic techniques, e.g., Raman or photoluminescence (PL) spectroscopies, are more widely used in that case. [13] PL experiments supported with DFT calculations reveal that V_S lead to the formation of nonzero density of states in the bandgap. [7,13-17] Low-temperature PL spectra show an additional low energy peak in ML MoS₂ flakes, which originates from bound excitons formed by localizing excitons at the defect sites, leading to emission energies that are lower than the band-to-band optical transition. [14] Such additional PL peak is generally observed in different TMDCs and it is attributed to the optical transitions from discrete energy levels of lattice defects (e.g., vacancies) or residual impurities introduced by ion irradiation or plasma treatments.^[14–16] However, bound excitons have also been observed in PL spectra of as-grown and mechanically exfoliated pristine ML WS₂ at room temperature. [17] Application of the DLTS technique for studying defects

directly in 2D semiconductors may require construction of suitable vdW heterostructures composed of ML flakes of different materials. [18,19] However, the lack of the space charge depletion/accumulation region in nanometer size devices, due to the lack of physical material space in the vertical direction, can make DLTS measurements difficult or even impossible to perform. Atomically thin vertical and asymmetric p-n junctions constructed of two vdW-bonded semiconductor layers can exhibit good rectifying properties. However, the underlying microscopic processes can differ strongly from those of conventional bulk devices in which an extended depletion region plays a crucial role. In particular, tunneling-mediated recombination occurs between majority charge carriers across the interface, which can significantly influence electrical and optoelectronic properties of the junction, as demonstrated for MoS₂/WSe₂ heterostructures.[20]

Due to many discrepancies in previously reported results, further efforts should be made for better understanding and control of structural defects in TMDC crystals. Such knowledge constitutes a key approach for controlling the transport characteristics and electrooptical properties of modern TMDC-based devices. Therefore, it is evident that further investigation of defects is a crucial step for 2D materials research and applications. In this article, we report on DLTS experiments conducted on MoS₂ bulk crystal, supported by electrical characterization of metal contacts and supplemented by optical measurements and first-principles calculations of electronic band structure.

Samples used for the studies were thick flakes of macroscopic sizes of about $3\times 4\,\mathrm{mm}$ in hexagonal plane and thickness $\approx 0.2\,\mathrm{mm}$ perpendicular to the hexagonal plane, thus the studied crystal consists of many of S–Mo–S strong covalently bonded atomic layers, which are, in turn, bonded by weak vdW forces between each other. Figure 1 shows schematic diagram and the real photo of the studied MoS_2 crystal with deposited circular metal contacts for electrical measurements.

Synthesized MoS_2 crystals were initially characterized by temperature-dependent current-voltage (I–V) and capacitance-voltage (C–V) measurements (see Supporting Information for more details), to select diodes with good electrical properties, appropriate for DLTS measurements. Comparative studies of circular Au contacts with bulk MoS_2 revealed a temperature-dependent ideality factor, Schottky barrier height (SBH), and series resistance. The results showed that while ideality factor and series resistance values of the junction decrease, the SBH values increase with the increase in temperature. The observed

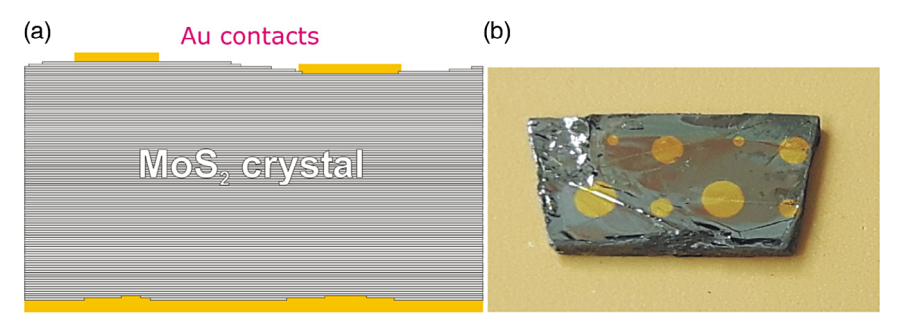


Figure 1. a) Schematic cross-sectional diagram of layers in the MoS₂ bulk crystal with deposited gold (Au) metal contacts; b) real photo of the studied sample.



SBH inhomogeneities are probably related to native sulfur defects present at the metal– MoS_2 interface. $^{[21,22]}$ On the contrary, the natural doping concentration in the studied MoS_2 vdW crystal was almost uniform for the whole measured temperature range. According to the preliminary electrical measurements, selected small circular Au/MoS_2 junction (0.3 mm in diameter) generally shows reasonable rectifying properties, which are applicable for further studies of deep-level defects by means of space charge techniques. Next, DLTS technique was used to probe electrically active defects with deep energy levels in the MoS_2 bandgap.

The fundamental electrical parameters of defects: the thermal activation energy ($E_a = E_{C,V} \pm E_T$), i.e., the deep energy level position (E_T) in the bandgap in relation to the conduction (E_C) or valence (E_V) band edges and the apparent capture cross section (σ_a), were determined on the basis of the well-known formula^[23]

$$e_{\rm n,p} = \sigma_{\rm a} \nu_{\rm th} N_{\rm C,V} \exp[-E_{\rm a}/k_{\rm B}T] \tag{1}$$

where $e_{\rm n,p}$ is the thermal emission rate for electrons/holes from a corresponding deep energy level into the conduction or valence band at temperature T, $\nu_{\rm th}$ is the thermal velocity of electrons/holes, $N_{\rm C,V}$ is an effective density of states in the conduction or valence band, and $k_{\rm B}$ is the Boltzmann's constant. Considering that $\nu_{\rm th} \propto T^{1/2}$ and $N_{\rm C,V} \propto T^{3/2}$ and assuming the temperature independence of the capture cross section, the Equation (1) becomes a linear equation in the $\ln(e_{\rm n,p}/T^2)$ versus 1000/T plot, called the Arrhenius plot. Arrhenius plots of defects are obtained by measuring a shift in the DLTS temperature peak position as a function of an emission rate. The thermal activation energy and capture cross section for each deep-level defect are determined from the slope and intercept values of the corresponding Arrhenius plot.

Standard DLTS spectrum, taken in the temperature range of $80{\text -}400~\text{K}$ for the MoS_2 crystal, is shown in **Figure 2**. The DLTS measurements were performed at the constant reverse bias (U_R) of -1~V and with the filling pulse bias (U_P) of 0~V, which corresponds to the estimated depletion layer width in the studied MoS_2 crystal at about $0.214~\mu\text{m}$ at 300~K. The emission rate

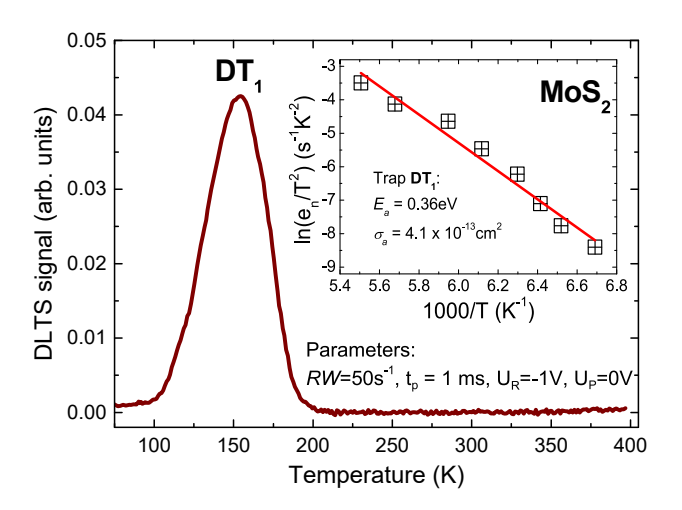


Figure 2. Standard DLTS spectrum obtained for MoS_2 crystal. The inset shows Arrhenius plot and obtained parameters of the trap labeled DT_1 .

window (RW) was set to $50 \, \mathrm{s}^{-1}$ and the width of the filling pulse (t_p) was equal to 1 ms. For these measurement conditions, a single positive peak labeled DT₁ was detected at about 153 K. The Arrhenius plot, shown in the inset of Figure 2, enabled us to calculate the thermal activation energy and apparent capture cross section of the revealed trap, at about 0.36 eV and $4.1 \times 10^{-13} \, \mathrm{cm}^2$, respectively. Moreover, the concentration (N_T) of the trap DT₁ equals to about $5 \times 10^{13} \, \mathrm{cm}^{-3}$ was determined from the magnitude of the DLTS peak, including the so-called λ -correction, in the way shown in our previous work. [24]

We postulate that the physical origin of the revealed defectinduced deep energy level is most probably attributed to sulfur vacancies (V_s) . There are at least several key reports which can support this assumption. First of all, the presence of high density of S-vacancies has been previously demonstrated in MoS₂ by means of TEM^[7,10,11] or scanning tunneling microscopy $(STM)^{[12]}$ observations. The V_S concentration in mechanically exfoliated samples or grown by chemical vapor deposition (CVD) or physical vapor deposition (PVD) techniques usually reaches $\approx 10^{11} - 10^{13} \text{ cm}^{-3}$. [10–12] Second, after introducing S-vacancies in MoS2 deep energy states can be formed with strong localization surrounding the vacancy. [11] The evidence of existence of defect-related energy levels has already been confirmed only by optical spectroscopic measurements (e.g., Raman or PL spectroscopy) for many 2D TMDCs, such as ML MoS₂, WSe₂, or WS₂.^[13–17] It is generally known that ML TMDCs have strong PL signals at room temperature due to the direct bandgap emissions. Namely, the Coulomb interaction between one electron and one hole creates so-called free neutral exciton (X₀). In addition, exciton can be further charged by binding an additional electron or hole to form the so-called charged three-body excitons named trions (X₀⁻, X₀⁺).^[13] Moreover, in addition to exciton and trion emissions, another PL emission (XB) can be observed, resulting from exciton bound to energy states of defects within the bandgap. Tongay et al. [14] found a subbandgap emission peak in low-temperature PL spectra of defective MoS₂, and also WSe₂ and MoSe₂ MLs after α-particle irradiation, which was not observed in the pristine samples. After calculating the band structure and the density of states of defective ML MoS₂, they attribute the defect-induced PL peak to the emission from energy levels of S-vacancies at \approx 0.2 eV above valence band maximum (VBM) or $\approx 0.3 \, \text{eV}$ below the conduction band maximum (CBM). Chow et al.^[15] also observed similar defect-induced PL peak in WS₂ and MoS₂ MLs after simple plasma treatments. However, in contrast to the previous results, [14] they observed such spectral feature with sufficient strength in air at room temperature and atmospheric pressure. Two defect-activated PL emission peaks were, in turn, observed by Wu et al. [16] in the low-temperature PL spectra of ML WSe₂ treated with Ar⁺ plasma. The observed emissions were attributed by the authors to the recombination of excitons bound to different types of native defects, namely, the shallow level to chalcogen vacancies and the deep level to transition metal vacancies, clusters of vacancies, rational defects, or antisite defects in ML WSe2. Defectrelated PL emission was also detected by McCreary et al. [17] in some exfoliated but not irradiated WS2 flakes. After irradiation with low energy Ar⁺ ion beam of other as-grown and exfoliated pristine WS2 samples, such peak also appeared as a result of defects creation by the irradiation process. Third, numerous

first-principles calculations predict the existence of native defects in ML and bulk MoS₂, or other TMDCs. $^{[7-10]}$ It was found that V_S manifest considerably lower formation energy compared with that of the Mo-vacancies (V_{Mo}) or other native defects and impurities, so they can be formed easily. DFT calculations performed by Qiu et al. [11] for ML MoS₂, in the presence of V_S , indicated the introduction of defect states at about 0.46 eV below CBM which act as deep electron donors to make the MoS2 electron rich and enable hopping transport at low carrier density regime. On the contrary, Noh et al. [8] found that V_S is a deep single acceptor with the (0/-1)transition level at 1.7 eV above the VBM (results obtained for calculated direct bandgap of MoS2 at K point with the value of 1.851 eV) and with the low formation energy at \approx 1 eV in Mo-rich conditions. They concluded that V_S cannot be efficient source of electron carriers in MoS₂ as previously reported, ^[11] but it can still act as electron trap center in n-type MoS₂. Similar results were also obtained by Komsa et al., [9] who performed detailed DFT studies of native defects in bulk and ML MoS2. Their calculations revealed that both S and Mo vacancies are always acceptors and thus cannot be the cause of the usually observed n-type doping of MoS₂. The $V_{\rm S}$ were found to be the most abundant defects with the (0/-1)transition level located at 0.29 eV below CBM in ML MoS2 and 0.31 eV below CBM in bulk MoS₂. The aforementioned experimental and theoretical results confirm the existence of V_s-related deep-level states in the bandgap of bulk and ML MoS2 with the energy-level position close to the one obtained here by DLTS for the deep trap DT₁. Despite the fact that most of the presented results were applied for ML MoS₂, there are also plenty of evidences that V_S should behave very similar both in the ML and in the bulk TMDCs crystals.^[8] Therefore, electrically active native defects revealed in bulk crystals should also be active in 2D TMDCs samples. It is obvious that activation energies of defects present in MLs should differ from those expected for bulk crystals due to different bandgaps. However, as shown here, the reported positions of V_s-related electron trap in the bandgap of ML or bulk TMDCs and obtained from PL or DFT are in a similar range of values. On the basis of these findings we can now conclude that the DT_1 trap is most probably associated with V_S being partially responsible for the observed temperature-dependent electrical properties of Au/MoS_2 junction.

The position of DT₁ trap on the electronic band structure of MoS2 is shown in Figure 3a. As the accuracy of bandgap calculations within DFT calculations is not high, the obtained electronic structure has been fitted to experimental data, i.e., measurements of the indirect gap by absorption and the direct optical transitions by contactless electroreflectance (CER). In this case, the fitting corresponds to a shift of conduction bands versus the valence band by 0.25 eV. Figure 3b shows absorption and CER spectrum measured for MoS₂ sample at room temperature. The indirect gap is determined from $\sqrt{\alpha}$ plot to be 1.37 eV. In case of CER spectrum, the indirect gap is not observed and only direct optical transitions are visible because of differential character of this technique. Spectral features observed in CER spectrum have been fitted by Aspnes formula^[25] and identified according to recent studies. [26] The A and B transitions are marked in Figure 3a by proper arrows and their energies agree very well with experimental data. The A_H transition is the direct optical transition at the H point of Brillouin zone, [26] which is not shown in Figure 3a. According to DLTS study, the position of sulfur vacancy is located at about 0.36 eV below the conduction band minimum, which is between the K and Γ point of Brillouin zone. In Figure 3a, the energy position of DT₁ is schematically shown by dashed olive line.

In summary, deep-level defects were studied by means of DLTS technique in bulk MoS₂ vdW crystal. DLTS temperature spectrum measured for one of the Au/MoS₂ Schottky diodes revealed a single deep-level trap with activation energy of 0.36 eV below CBM. The position of the deep trap is very close to the value both theoretically predicted and experimentally confirmed for discrete energy levels that are introduced by the

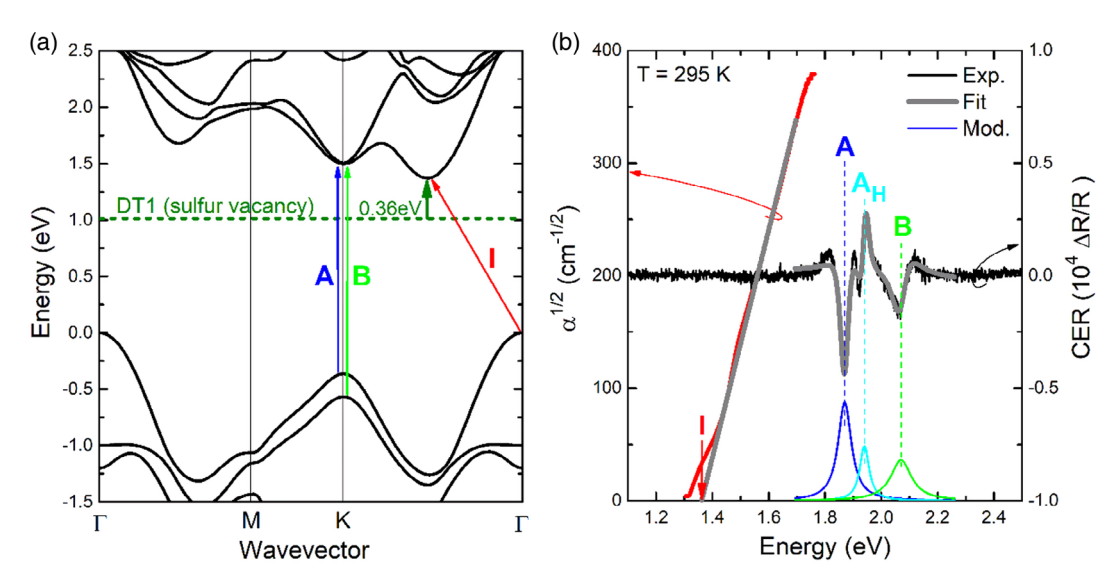


Figure 3. a) Electronic band structure of MoS_2 calculated within the DFT with marked optical transitions observed in absorption and CER measurements. The energy position of sulfur vacancy on the electronic band structure of MoS_2 is shown by dashed olive line. b) Room temperature absorption spectrum (red curve) and CER spectrum (black curve). CER spectrum is fitted by Aspnes formula (thick gray line) with three optical transitions. Moduli of the optical transitions are plotted by color lines.



www.advancedsciencenews.com



www.pss-rapid.com

sulfur vacancies. Therefore, we concluded that the trap is attributed to V_S being partially responsible for the observed temperature-dependent electrical properties of Au/MoS_2 junction (additionally presented in Supporting Information).

Experimental Section

The studied MoS₂ crystal was fabricated by iodine-assisted vapor transport technique at high temperatures (900–1100 °C) and low pressure ($\approx 1 \times 10^{-6}\, \text{Torr}$) in a sealed quartz ampoule. During the growth at $\approx \!50\,^{\circ}\,\text{C}$, temperature differential was created between hot and cold zones to initiate nucleation and facilitate precursor transport. Prior to the growth, quartz ampoules ($\approx \!15\,\text{cm}$ in length, 2.4 cm outer diameter, and 2.0 cm inner diameter) were cleaned in piranha solution and annealed in H₂ gas to remove any contaminants. Precursors (Mo foils and S nuggets) were mixed in 1:2.05 M:X stoichiometric ratio, and iodine pieces were added as a transport agent. Quartz ampoule is sealed under vacuum (1 $\mu Torr$).

The electrical measurements were performed within the wide temperature range from 80 to 450 K, with the use of Keithley 2601A source-meter and Boonton 7200 capacitance bridge (operating at 1 MHz), respectively. The samples were equipped with circular Au contacts with specific diameters equal to 0.1, 0.3, 0.5, and 0.8 mm on the top side of the sample (see Figure 1b). These contacts were deposited in vacuum through shadow mask by electrolithography technique and were intended to act as Schottky barrier contacts. Prior to the Schottky contact formation, the back contact was also deposited by Au metallization on a whole back side of the sample and additional annealing at 350 °C in the Ar atmosphere for 5 min. Thus, the large area back contact (\approx 12 mm²) ensures nonrectifying electrical conductivity with low resistance (i.e., ohmic behavior). The DLTS experiments were performed on the samples mounted in a liquid nitrogen cooled Janis VPF-475 cryostat. During measurements, temperature of the sample was precisely tuned by Lakeshore 331 temperature controller, in the range of 80-450 K.

The electronic band structure of MoS₂ crystal has been calculated within the DFT according to the state of the art for vdW crystals. The calculations were performed with ABINIT code.^[27] In the first step, the structure was optimized, with the use of projector augmented wave (PAW) datasets for atoms representation^[28] joined with the generalized gradient approximation (GGA) proposed by Perdew, Burke, and Ernzerhof (PBE) for exchange-correlation (XC) energy functional. [29] The vdW interaction has been accounted for via the vdw-DFT-D3 correction as proposed by Grimme. $^{[30]}$ The computational parameters energy cutoff 30 Ha and special k-points grid 8 × 8 × 6 have been applied. The obtained lattice parameters are: a = 5.971 Bohr and c = 23.171 Bohr, and the atomic positions optimized down to maximum force 10^{-7} Ha Bohr⁻¹. The band structure has been calculated with the use of norm-conserving pseudopotentials, generated with atomic pseudopotential engine (APE) code, [31] joined with the modified Becke-Johnson local density approximation (mBJLDA) XC-functional^[32] with computational parameters chosen after careful convergence studies, and with standard convergence criteria.

Absorption and CER spectroscopy were applied to measure the indirect gap and the direct optical transitions in MoS₂. For absorption measurements, both the reflectance and transmittance spectrum were measured using a setup with a halogen lamp, 0.3 m monochromator, and Si detector. The same setup was used to measure CER spectra. For CER measurements, the sample was placed in a capacitor with a half-transparent top electrode. The distance between the sample surface and the semitransparent electrode was 0.5 mm. A maximum peak-to-peak alternating voltage of 3.5 kV with the frequency of 280 Hz was used for the modulation. The CER signal was measured using lock-in technique. Other relevant details of CER measurements are described elsewhere. [33]

Supporting Information

Supporting Information is available from the Wiley Online Library or from the author.

Acknowledgements

This work was supported by the National Science Centre (NCN), Poland OPUS 13 Grant No. 2017/25/B/ST7/01203 and Wrocław University of Science and Technology statutory grant. S.T. acknowledges support from NSF DMR-1552220 and NSF DMR-1955889 and NSF-CMMI 1933214.

Conflict of Interest

The authors declare no conflict of interest.

Keywords

deep-level transient spectroscopy, MoS_2 , native defects, van der Waals crystals

Received: August 6, 2020 Revised: September 7, 2020 Published online: September 22, 2020

- Q. H. Wang, K. Kalantar-Zadeh, A. Kis, J. N. Coleman, M. S. Strano, Nat. Nanotechnol. 2012, 7, 699.
- [2] D. Jariwala, V. K. Sangwan, L. J. Lauhon, T. J. Marks, M. C. Hersam, ACS Nano 2014, 8, 1102.
- [3] W. Choi, N. Choudhary, G. H. Han, J. Park, D. Akinwande, Y. H. Lee, Mater. Today 2017, 20, 116.
- [4] D. Voiry, A. Mohite, M. Chhowalla, Chem. Soc. Rev. 2015, 44, 2702.
- [5] K. F. Mak, C. Lee, J. Hone, J. Shan, T. F. Heinz, Phys. Rev. Lett. 2010, 105, 136805.
- [6] Z. Lin, B. R. Carvalho, E. Kahn, R. Lv, R. Rao, H. Terrones, M. A. Pimenta, N. Terrones, 2D Mater. 2016, 3, 022002.
- [7] W. Zhou, X. Zou, S. Najmaei, Z. Liu, Y. Shi, J. Kong, J. Lou, P. M. Ajayan, B. I. Yakobson, J.-C. Idrobo, *Nano Lett.* 2013, 13, 2615.
- [8] J.-Y. Noh, H. Kim, Y.-S. Kim, Phys. Rev. B 2014, 89, 205417.
- [9] H. P. Komsa, A. V. Krasheninnikov, Phys. Rev. B 2015, 91, 125304.
- [10] J. Hong, Z. Hu, M. Probert, K. Li, D. Lv, X. Yang, L. Gu, N. Mao, Q. Feng, L. Xie, J. Zhang, D. Wu, Z. Zhang, C. Jin, W. Ji, X. Zhang, J. Yuan, Z. Zhang, Nat. Commun. 2015, 6, 6293.
- [11] H. Qiu, T. Xu, Z. Wang, W. Ren, H. Nan, Z. Ni, Q. Chen, S. Yuan, F. Miao, F. Song, G. Long, Y. Shi, L. Sun, J. Wang, X. Wang, Nat. Commun. 2013, 4, 2642.
- [12] S. McDonnell, R. Addou, C. Buie, R. M. Wallace, C. L. Hinkle, ACS Nano 2014, 8, 2880.
- [13] Z. Wu, Z. Ni, Nanophotonics 2017, 6, 1219.
- [14] S. Tongay, J. Suh, C. Ataca, W. Fan, A. Luce, J. S. Kang, J. Liu, C. Ko, R. Raghunathanan, J. Zhou, F. Ogletree, J. Li, J. C. Grossman, J. Wu, Sci. Rep. 2013, 3, 2657.
- [15] P. K. Chow, R. B. Jacobs-Gedrim, J. Gao, T.-M. Lu, B. Yu, H. Terrones, N. Koratkar, ACS Nano 2015, 9, 1520.
- [16] Z. Wu, W. Zhao, J. Jiang, T. Zheng, Y. You, J. Lu, Z. Ni, J. Phys. Chem. C 2017, 121, 12294.
- [17] A. McCreary, A. Berkdemir, J. Wang, M. A. Nguyen, A. L. Elías, N. Perea-López, K. Fujisawa, B. Kabius, V. Carozo, D. A. Cullen, T. E. Mallouk, J. Zhu, M. Terrones, J. Mater. Res. 2016, 31, 931.
- [18] K. S. Novoselov, A. Mishchenko, A. Carvalho, A. H. Castron Neto, Science 2016, 353, aac9439.
- [19] M. Velický, P. S. Toth, Appl. Mater. Today 2017, 8, 68.
- [20] C.-H. Lee, G.-H. Lee, A. M. van der Zande, W. Chen, Y. Li, M. Han, X. Cui, G. Arefe, C. Nuckolls, T. F. Heinz, J. Guo, J. Hone, P. Kim, Nat. Nanotechnol. 2014, 9, 676.



www.advancedsciencenews.com



- [21] F. Giannazzo, G. Fisichella, A. Piazza, S. Agnello, F. Roccaforte, Phys. Rev. B 2015, 92, 081307.
- [22] M. Moun, R. Singh, Semicond. Sci. Technol. 2018, 33, 125001.
- [23] P. Blood, J. W. Orton, The Electrical Characterization of Semiconductors: Majority Carriers and Electron States, Academic Press, London, UK 1992.
- [24] Ł. Gelczuk, J. Kopaczek, T. B. O. Rockett, R. D. Richards, R. Kudrawiec, Sci. Rep. 2017, 7, 12824.
- [25] D. E. Aspnes, Surf. Sci. 1973, 37, 418.
- [26] J. Kopaczek, M. P. Polak, P. Scharoch, K. Wu, B. Chen, S. Tongay, R. Kudrawiec, J. Appl. Phys. 2016, 119, 235705.
- [27] X. Gonze, B. Amadon, P.-M. Anglade, J.-M. Beuken, F. Bottin, P. Boulanger, F. Bruneval, D. Caliste, R. Caracas, M. Côté,
- T. Deutsch, L. Genovese, P. Ghosez, M. Giantomassi, S. Goedecker, D. R. Hamann, P. Hermet, F. Jollet, G. Jomard, S. Leroux, M. Mancini, S. Mazevet, M. J. T. Oliveira, G. Onida, Y. Pouillon, T. Rangel, G.-M. Rignanese, D. Sangalli, R. Shaltaf, M. Torrent, et al., *Comput. Phys. Commun.* **2009**, *180*, 2582.
- [28] P. E. Blöchl, Phys. Rev. B 1994, 50, 17953.
- [29] J. P. Perdew, K. Burke, M. Ernzerhof, Phys. Rev. Lett. 1997, 78, 1396.
- [30] S. Grimme, J. Antony, S. Ehrlich, H. Krieg, J. Chem. Phys. 2010, 132, 154104.
- [31] M. J. T. Oliveira, F. Nogueira, Comput. Phys. Commun. 2008, 178, 524.
- [32] F. Tran, P. Blaha, Phys. Rev. Lett. 2009, 102, 226401.
- [33] R. Kudrawiec, W. Walukiewicz, J. Appl. Phys. 2019, 126, 141102.